

Higgs boson in a flavor-extension of the CMSSM

Surabhi Gupta^{a1}, Sudhir Kumar Gupta^{a2}, and Keven Ren^{b3}

^a*Department of Physics, Aligarh Muslim University, Aligarh, UP-202002, India*

^b*School of Physics and Astronomy, Monash University, Melbourne, Victoria 3800, Australia*

Abstract

Flavour-violating couplings of Higgs boson with stop and scharm quarks could be very important as in addition to lifting the mass of the Higgs boson by a few GeV, it could also play a vital phenomenological role in reducing the Supersymmetry breaking scale significantly. In this work, we investigate effects of such flavour-violating couplings within the Constrained Minimal Supersymmetric Standard Model (CMSSM) framework in the context of LEP data, Higgs data at the LHC, precision observables and the relic density of the dark matter using Bayesian statistics. Our detailed analysis reveals that the most probable values of m_0 , $m_{1/2}$, A_0 , $\tan\beta$, δ_{ct}^{LR} are expected to be around 4.83 TeV, 2.54 TeV, 1.90 TeV, 41.5, and 6.1×10^{-2} , respectively, with flat priors. The corresponding values translate into 3.25 TeV, 2.13 TeV, 1.90 TeV, 44.7, and 5.9×10^{-2} , respectively, if the natural priors are used. Furthermore, a comparison of our model with the CMSSM of flavour-conservation as the base model yields a Bayes factor of about 6 while taking into account all the experimental constraints used in our study. Our analysis also reflects that the lightest neutralino would have a mass of about 1 TeV.

¹E-mail:sgupta2@myamu.ac.in

²E-mail:sudhir.ph@amu.ac.in

³E-mail:Keven.Ren@monash.edu

1 Introduction

Within the Standard Model (SM) [1], the Higgs mechanism is the underlying mechanism allowing for the electroweak (EW) symmetry breaking and thus generation of masses for the elementary particles. The resulting postulate of a scalar fundamental particle is one of the major reasons for construction of the Large Hadron Collider (LHC). In 2012, the ATLAS and CMS collaborations have recorded the observation of a spin-zero particle with qualities consistent with that of the Higgs boson [2]. Under the Constrained Minimal Supersymmetric Standard Model (CMSSM) [3–9] framework, only five parameters are required to generate the supersymmetric spectrum. However, it remains difficult for CMSSM to justify a Higgs mass of 125 GeV with reasonable assumptions. Recent experimental results for the non-observance of a supersymmetric particle below 1 TeV bring additional stress to the theory as the little hierarchy issue becomes more prominent with heavier stops. The amount of fine-tuning required increases with the energy gap between the Supersymmetry (SUSY) [10–18] breaking scale and the EW regime. Therefore, it is desirable to search beyond the SM phenomenon which may propose alternative solutions to accommodate a Higgs mass of 125 GeV without stretching this gap. Models such as Peccei-Quinn extension to the SM [19] and non-minimal flavour violation (NMFV) [20–37] are examples of methods one may utilise to explain a 125 GeV Higgs mass. The first work on NMFV has been presented in Ref. [20], where the authors have studied the effects of NMFV in the MSSM involving up-type squarks of the second and third generation in the left-left (LL) sector and have shown contributions to the electroweak observables and the lightest MSSM Higgs boson mass. Another work has been published in Ref. [21] about the contributions of the NMFV SUSY in context of the hadroproduction and decay of sparticles. In a work by Arana-Catania et al. [22–24], the authors have contended that flavour-changing couplings, particularly within the scharm-stop sector, have the capacity to increase the Higgs mass by up to 10 GeV. The additional flavour-violating interactions are also expected to reduce the unified masses, therefore bringing the squark masses closer to the EW scale. The connection has been beheld between the flavour-violating terms of the squark and the slepton sectors at the Grand Unified Theory (GUT) and the TeV scale in the NMFV SUSY framework [25]. Additional works in NMFV have been implemented in other directions including Higgs boson decays [33], Gauge-mediated SUSY Breaking (GMSB) model [34], Anomaly-mediated SUSY Breaking (AMSB) model [35], Z_3 invariant Next-to MSSM (NMSSM) scenario [36], and CMSSM model [37]. Flavour-changing neutral-current process [13] similar to the NMFV context has been explored in the hybrid gauge-gravity model [38] and the top-quark processes at the LHC [39–41]. Significant contribution of the supersymmetric particles towards the decays of flavour-changing neutral MSSM Higgs bosons to the second and third generation quarks has also been studied in Refs. [42–44]. Motivated by the premise of Arana-Catania et al., we investigate a CMSSM scenario extended with non-minimal flavour-violating interaction and then compare it with the vanilla CMSSM case. Both models are subjected to various experimental constraints and good fitting regions of the parameter space are found and compared. A Bayesian analysis is then provided to give a quantitative basis for the plausibility of the models against each other.

The rest of the paper is organised as follows. Section II discusses the NMFV extension to CMSSM. Section III includes our method, Bayes statistics and the constraints applied. Section IV gives the detailed results and Bayesian analysis. Section V is the conclusion.

2 Flavour–violation in MSSM and the Higgs boson

Within MSSM the flavour-violating terms could typically arise due to the RG flow of various squark masses from the SUSY-breaking scale down to the EW scale. However such terms are heavily suppressed. Under the NMFV scheme, the off-diagonal flavour-violating terms of the squark mass matrices under the super-CKM basis are not suppressed at lower energy scales, particularly in the top-charm sector [45]. Therefore, considering the flavour violation in the top-charm sector, which could possibly give rise to a few extra GeV contribution to the Higgs boson mass and thus reduce the SUSY-breaking scale significantly. The mass matrices of the up-type squarks could be described as

$$\mathcal{M}_{\tilde{U}_X}^2 = \begin{pmatrix} M_{\tilde{U}_{X11}}^2 & 0 & 0 \\ 0 & M_{\tilde{U}_{X22}}^2 & \delta_{23}^{XX} M_{\tilde{U}_{X22}} M_{\tilde{U}_{X33}} \\ 0 & \delta_{23}^{XX} M_{\tilde{U}_{X22}} M_{\tilde{U}_{X33}} & M_{\tilde{U}_{X33}}^2 \end{pmatrix}, \quad (1)$$

with the up-type trilinear coupling in terms of flavour-violating off-diagonal terms could be given as

$$v_1 \mathcal{A}^u = \begin{pmatrix} 0 & 0 & 0 \\ 0 & 0 & \delta_{ct}^{LR} M_{\tilde{U}_{L22}} M_{\tilde{U}_{R33}} \\ 0 & \delta_{ct}^{RL} M_{\tilde{U}_{R22}} M_{\tilde{U}_{L33}} & m_t A_t \end{pmatrix}. \quad (2)$$

In Eq. (1), the dimensionless coefficient δ_{ij}^{XY} is the flavour-violating coupling where X is either chiral L (left) or R (right), i, j represent the generations of the squarks, and $M_{\tilde{U}_{Xij}}$ is the up-type squark mass. In Eq. (2), v_1 is the vacuum expectation value (VEV) of the H_u , matrix \mathcal{A}^u includes values of the Yukawa-type couplings of the Higgs and the up-type squarks, m_t denotes the top-quark mass, and A_t represents the trilinear coupling of the stop. The corresponding down-type mass matrices $\mathcal{M}_{\tilde{D}_X}^2$ and down-type trilinear coupling $v_2 \mathcal{A}^d$, where v_2 represents the VEV of the H_d and matrix \mathcal{A}^d includes values of the Yukawa-type couplings of the Higgs and the down-type squarks, completely analogous to Eqs. (1) and (2), respectively and could be found by replacing the respective indices. The contributions towards the Higgs masses are expected to occur in the LR/RL category, as the flavour-violating coupling is now being factored directly into the Yukawa-type coupling involving the Higgs boson and squarks [22–24]. The suppression of flavour-violating interaction involving the first generation squarks is due to existing experimental data already restricting its possible range. In this investigation, only the NMFV effects in the second and third generation squarks in the LR sector are considered due to the most significant contribution provided to the Higgs mass. As a result the SUSY breaking scale is significantly reduced relative to the RL, LL , and RR sectors. In [45], the extent of FV within the top-charm sector has been constrained to $|\delta_{ct}^{XY}| \lesssim 0.5$ at a 1σ confidence level using the measurements on the decay width of top-quark, $\Gamma_t = 1.42_{-0.15}^{+0.19}$ GeV [46]. In the context of the CMSSM the flavour-violating coupling appears in the one-loop correction to the Higgs mass, which can be expressed as

$$\Delta m_h(\delta_{ct}^{LR}) \equiv m_h^{NMFV}(\delta_{ct}^{LR}) - m_h^{CMSSM}, \quad (3)$$

where $\Delta m_h(\delta_{ct}^{LR})$ is the correction to the Higgs mass due to the inclusion of flavour-violating coupling. If $\delta_{ct}^{LR} = 0$ then this correction vanishes: $m_h^{NMFV}(\delta_{ct}^{LR}) = m_h^{CMSSM}$. In this work we use `FeynHiggs` [48–55] for the numerical computation of the parameters $m_h^{NMFV}(\delta_{ct}^{LR})$ and m_h^{CMSSM} . Further details on Eq. (3) can be found in Refs. [22–24].

3 Numerical analysis

We use a Bayesian analysis to quantitatively evaluate the plausibility of our model. Comparing theoretical predictions of our model to experimental observations, we can determine regions in the parameter space where our model best agrees with the experiment. To this end, we introduce the likelihood function for a point $x = \{x_1, x_2, \dots, x_n\}$ in the parameter space as

$$\mathcal{L}_i(x) = \frac{1}{\sqrt{2\pi}\sigma_i} \exp\left(-\frac{\chi_i^2}{2}\right). \quad (4)$$

Here, for each observables \mathcal{O}_i , χ_i^2 is defined as

$$\chi_i^2 = \frac{(\mathcal{O}_i(x) - \mathcal{O}_i^{exp})^2}{\sigma_i^2}, \quad (5)$$

where \mathcal{O}_i^{exp} is the experimentally measured value of the observable, $\mathcal{O}_i(x)$ is the corresponding theoretical prediction calculated at a point in the parameter space, and σ_i is the corresponding uncertainty. The likelihood quantifies the agreement of the theoretical prediction with experiment. To include all observables considered in our analysis, as shown in Table 3, we formed the composite likelihood as the product of all \mathcal{L}_i ,

$$\mathcal{L} = \prod_i \mathcal{L}_i. \quad (6)$$

The posterior probability distribution of a given parameter $x_j \in x$ is calculated by marginalising over the rest of the parameter space,

$$\mathcal{P}(x_j) = \frac{\int \mathcal{L}^\xi \prod_{i \neq j} dx_i}{\mathcal{E}}, \quad (7)$$

where ξ denotes our selection of priors, and the evidence is defined as

$$\mathcal{E} = \int \mathcal{L}^\xi dx. \quad (8)$$

The evidence is essential for calculating the Bayes factor, Q_{Bayes} , which is a quantitative measure of the plausibility of the NMFV CMSSM compared to CMSSM without NMFV couplings. The Bayes factor is written as

$$Q_{Bayes} = \log_{10} \left(\frac{\mathcal{E}_{NMFV}}{\mathcal{E}_{CMSSM}} \right). \quad (9)$$

We analyse the NMFV parameter space subjected to various constraints including LEP

Particle	Bound	Source
m_t	172.89 ± 0.59 GeV	[46]
m_h	> 114.4 GeV	[59]
$m_{\tilde{\chi}_1^0}$	$> \frac{m_Z}{2}$	[46]
$m_{\tilde{\chi}_1^\pm}$	> 103.5 GeV	[46]

Table 1: LEP bounds on Higgs and sparticles masses.

Constraint	Observable	Quantity	Source
Higgs observables (HO)	m_h	125.09 ± 0.24 GeV	[2]
	$\mathcal{R}_{gg\gamma\gamma}$	1.11 ± 0.10	[46]
	$\mathcal{R}_{gg2l2\nu}$	1.19 ± 0.12	[46]
	\mathcal{R}_{gg4l}	1.20 ± 0.12	[46]
	\mathcal{R}_{ggbb}	1.04 ± 0.13	[46]
	$\mathcal{R}_{gg\tau\tau}$	1.15 ± 0.16	[46]
Precision observables (PO)	$\Delta\rho$	0.00038 ± 0.0002	[46]
	Δa_μ	$(2.51 \pm 0.59) \times 10^{-9}$	[60]
	$Br(b \rightarrow s\gamma)$	$(3.32 \pm 0.15) \times 10^{-4}$	[46, 61]
Dark matter (DM)	$\Omega_\chi h^2$	0.1197 ± 0.0022	[62]

Table 2: List of experimental observables applied in our analysis.

data on Higgs mass and sparticles masses, Higgs observables, precision observables, and the abundance of dark matter at a 2.5σ confidence level. Details of these constraints and their experimental values can be found in Tables 1 and 2. The experimental data account for the Higgs observables [2, 46] obtained from the ATLAS and CMS collaborations. The \mathcal{R} is the ratio of overall rate process of SUSY over SM counterpart.

The decay rate

$$\mathcal{R}_{gg\gamma\gamma} = \left[\frac{\sigma_{pp \rightarrow h} \times \Gamma^{h \rightarrow \gamma\gamma}}{\Gamma_h} \right]_{\frac{SUSY}{SM}} \quad (10)$$

is enhanced in supersymmetry, generating more $gg \rightarrow \gamma\gamma$ events than predicted by SM. We assume $\sigma_{pp \rightarrow h} \simeq \Gamma^{h \rightarrow gg}$ due to dominant Higgs production at the LHC by the gluon fusion. Above $\Gamma^{h \rightarrow \gamma\gamma}$ is the partial decay width, and Γ_h is the total decay width of Higgs boson. Similarly, the \mathcal{R} value can be evaluated for NMFV over its SM counterpart for the processes $gg \rightarrow \gamma\gamma$, $gg \rightarrow 2l2\nu$, $gg \rightarrow 4l$, $gg \rightarrow bb$ and $gg \rightarrow \tau\tau$.

4 Results and Discussions

In this section, we present our results in the form of the posterior probability distributions under various experimental constraints. The models examined in this discussion are cases of CMSSM with NMFV in the LR sector of the charm-stop flavour-violating interaction and CMSSM with no NMFV interactions. We examine our study only in the

scharm-stop sector as the contributions of couplings involving up-quark with top-quark or charm-quark are suppressed. Moreover, the coupling δ_{ct}^{LR} provides the most significant contribution to the Higgs mass as compared to other couplings like δ_{ct}^{RL} , δ_{23}^{LL} , and δ_{ct}^{RR} as discussed in Refs. [22–24] and also reduces the SUSY breaking scale significantly. The ATLAS and the CMS collaborations attained the combined mass measurement of the lightest Higgs boson as 125.09 ± 0.24 GeV [2]. Without modifications to CMSSM, the theory experiences difficulty in achieving this value without pushing the supersymmetric breaking scale to problematic ranges. We allude to this problem with the introduction of NMFV in the scharm-stop sector, where it can be seen to favourably impact the unified supersymmetric parameters. The 125 GeV Higgs mass can now be accomplished effortlessly following one-loop correction to the Higgs mass under the influence of NMFV coupling. In the calculation of the Bayes factor, the full scope of this study is included for brevity. Here we employ a random scan technique over the entire parameter space of CMSSM with NMFV as follows

- $m_0 \in [0.01, 6]$ TeV,
- $m_{1/2} \in [0.01, 6]$ TeV,
- $A_0 \in [-6, 6]$ TeV,
- $\tan\beta \in [0, 60]$,
- $\text{sgn}(\mu) = +1$,
- $\delta_{ct}^{RL} \in [-0.07, 0.07]$.

The parameters sample includes the usual five parameters of CMSSM, namely m_0 unified scalar mass, $m_{1/2}$ unified gaugino mass, A_0 common trilinear coupling parameter, $\tan\beta$ ratio of VEVs of up- and down-type Higgs bosons, $\left(\frac{v_1}{v_2}\right)$, and $\text{sgn}(\mu)$ sign associated with the Higgsino mass parameter μ along with a flavour-violating coupling δ_{ct}^{LR} . The entirety of the supersymmetric spectrum is created using these terms and the results are filtered using various experimental constraints.

Procuring the aforementioned parameters, we would use **Softsusy** [47] to generate the spectrum of supersymmetric particles. An additional parameter involved in this step is defining the mass of the top quark. **FeynHiggs** [48–55] is in conjunction with **Softsusy** [47] that is used in calculating the various Higgs observables such as masses, mixings, and branching ratios and ρ -parameter up to the two-loop level. **Superiso** [56] is used to calculate the relevant B-physics observables and the muon anomalous magnetic moment and, in addition, **micromegas** [57, 58] is employed to compute the relic density of the neutralino dark matter using the spectrum generator.

The variation of the CMSSM parameters against the posterior probability for flat priors, i.e., $\xi \propto 1$ and natural priors, $\xi \propto (m_0 m_{1/2})^{-1}$, respectively, taking into consideration the constraints of LEP data, Higgs observables, precision observables, and the relic density of the neutralino dark matter in the LR sector are presented in Figures 2 and 3. Taking note of the parameter, $\tan\beta$, the CMSSM case reveals a high preference in the value of $\tan\beta \approx 45$ with flat priors and ≈ 46 with natural priors which is expected as a higher $\tan\beta$ term contributes positively towards the Higgs mass. Comparatively, the reduced value of

$Q_{Bayes} = \log_{10} \left(\frac{\mathcal{E}_{NMFV}}{\mathcal{E}_{CMSSM}} \right)$		
LEP+HO	+PO	+DM
0.02	0.10	5.73
0.10	0.16	6.01

Table 3: Bayes factors in the NMFV scenario taking into account the experimental constraints with flat priors (first row) and natural priors (second row) for $m_0 \in [0.1, 4]$, $m_{1/2} \in [0.1, 4]$, $A_0 \in [-4, 4]$ (all in TeV units), $\tan \beta \in [0, 60]$, and $\delta_{ct}^{LR} \in [-0.07, 0.07]$.

favoured regions in the NMFV case for $\tan \beta \approx 42$ with flat priors and ≈ 45 with natural priors can be attributed to the phenomenon of NMFV supplementing the mass of the Higgs that allows for the likelihood of other regions to increase relatively. By comparing the two choices of models, it is apparent that both unified scalar and gaugino masses shift favourably towards the lower energy range for the NMFV case while both masses can be seen as naturally increasing. In the base CMSSM model, the expected values of m_0 , $m_{1/2}$, and A_0 are 5.98 TeV, 3.37 TeV, and -0.35 TeV, respectively, with flat priors while these values correspond to 6.00 TeV, 3.21 TeV, and -0.35 TeV, respectively, with natural priors. In NMFV the corresponding values of m_0 , $m_{1/2}$ and A_0 should be 4.83 TeV, 2.54 TeV, and 1.90 TeV, respectively, with flat priors and 3.25 TeV, 2.13 TeV, and 1.90 TeV, respectively, with natural priors. For the sake of deep understanding, Figures 1, 4–7 are presented with three different sets of constraints, i.e., (i) LEP+HO, (ii) LEP+HO+PO, and (iii) LEP+HO+PO+DM. It is to be noted that the likelihood of satisfying the observables peaks at $\delta_{ct}^{LR} \approx 6 \times 10^{-2}$ for flat as well as natural priors when all the constraints are included as shown in Figure 1. The most probable values of δ_{ct}^{LR} associated with different sets of constraints using flat and natural priors are presented in Table 4. These non-zero preferable peaks motivate the belief that the NMFV supplemented CMSSM is able to accommodate the addition of new physics under the constraints of experimental observables. However, we explore our study only with the LR sector of the scharm-stop flavour-violating interaction as giving the largest contribution to the Higgs mass relative to other flavour-violating couplings such as δ_{ct}^{RL} , δ_{23}^{LL} , and δ_{ct}^{RR} [22–24]. We present heatmaps of m_0 , $m_{1/2}$ and posterior probability bounded by the different sets of constraints in Figures 4 and 5 with flat and natural priors, respectively. Likewise, we also show heatmaps of sparticles mass with a posterior probability corresponding to flat and natural priors in Figures 6 and 7, respectively. The most probable masses of gluino, lighter stop, lighter stau, lighter chargino, and the lightest neutralino with flat priors taking into account all the above-mentioned constraints are 5.57 TeV, 5.14 TeV, 4.62 TeV, 1.07 TeV, and 1.04 TeV, respectively while these values are changed in natural priors by 4.54 TeV, 3.55 TeV, 2.47 TeV, 1.04 TeV, and 0.95 TeV, respectively. The most preferred values of various parameters in our work are listed in Table 4. It is to be noted that the other way to look at the most probable masses of m_0 , $m_{1/2}$ and sparticles can be found relatively well through heatmaps as indicated in Figures 4–7. The Bayes factors are found to be 5.73 with the flat priors and 6.01 with the natural priors after taking into account all the above-mentioned constraints, as illustrated in Table 3, predicting that the NMFV framework is strongly favoured against the CMSSM framework.

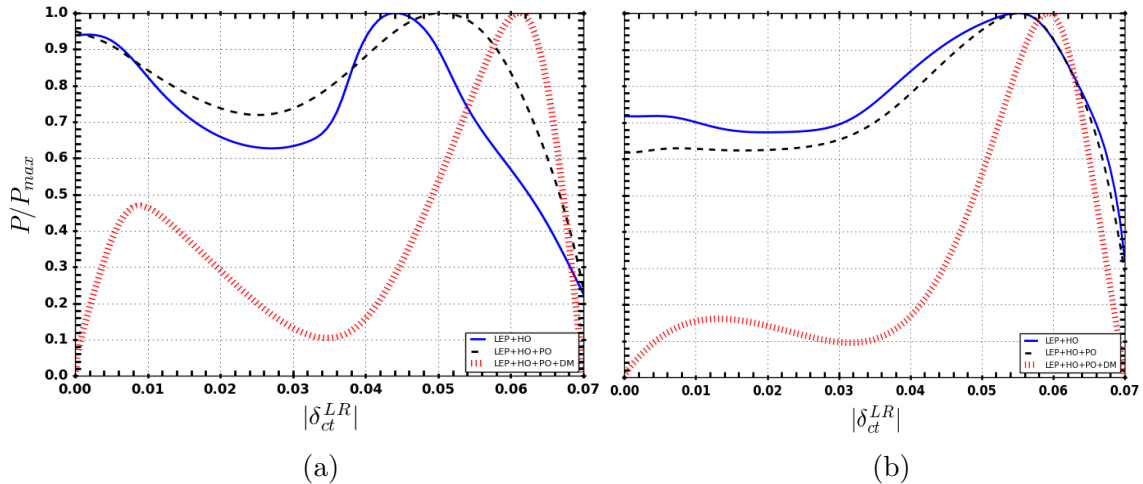


Figure 1: Posterior probability distributions of δ_{ct}^{LR} flavour-violating coupling of NMFV for different sets of constraints applied with (a) flat and (b) natural priors. The blue solid line indicates LEP data and Higgs observables constraints, the black dashed line signifies the constraints of LEP data, Higgs observables, and precision observables and the red dotted line includes the constraints of LEP data, Higgs observables, precision observables, and the relic density of the dark matter. The description of constraints is presented in Tables 1 and 2.

5 Summary

In this study, we have examined the effects of flavour-violating t-c interactions in the Constrained MSSM with the aid of Bayesian statistics. A detailed random scan over the CMSSM parameter space has been performed to explore the impact of such flavour-violating couplings by taking into account various experimental constraints arising from the LEP data, LHC data on Higgs, B-physics and electroweak precision observables, and the relic density of the dark matter. We have displayed the findings in Figures 1–7. Our work reveals that masses of the neutralino LSP, the lighter chargino, and gluino for the LR sector are found to be around 1.04 TeV, 1.07 TeV, and 5.57 TeV, respectively, with flat priors, whereas the corresponding masses are observed to be about 0.95 TeV, 1.04 TeV, and 4.54 TeV, respectively, with natural priors. Further, sfermion masses are observed to be in the range of 4.62 TeV to 7.13 TeV with the flat priors while these masses change with the natural priors in the range of 2.47 TeV to 4.63 TeV. The masses of other Higgses are found to be around 2 TeV corresponding to flat as well as natural priors. Exclusively this scenario assists to reduce the SUSY breaking scale, thus the most probable values of free CMSSM parameters m_0 , $m_{1/2}$, A_0 , $\tan\beta$, and NMFV coupling parameter δ_{ct}^{LR} are observed to be around 4.83 TeV, 2.54 TeV, 1.90 TeV, 41.5, and 6.1×10^{-2} , respectively, with flat priors while these values turn out to be 3.25 TeV, 2.13 TeV, 1.90 TeV, 44.7, and 5.9×10^{-2} , respectively, with natural priors at maximum posterior probability. The preferable values of δ_{ct}^{LR} are within top phenom constraints. The LHC Higgs mass constraint has favoured a small value to the flavour-violating coupling. The most probable values of sparticles masses, CMSSM input parameters and the NMFV coupling parameter in the allowed parameter space are displayed in Table 4. Other NMFV effects are noteworthy in the case of SUSY

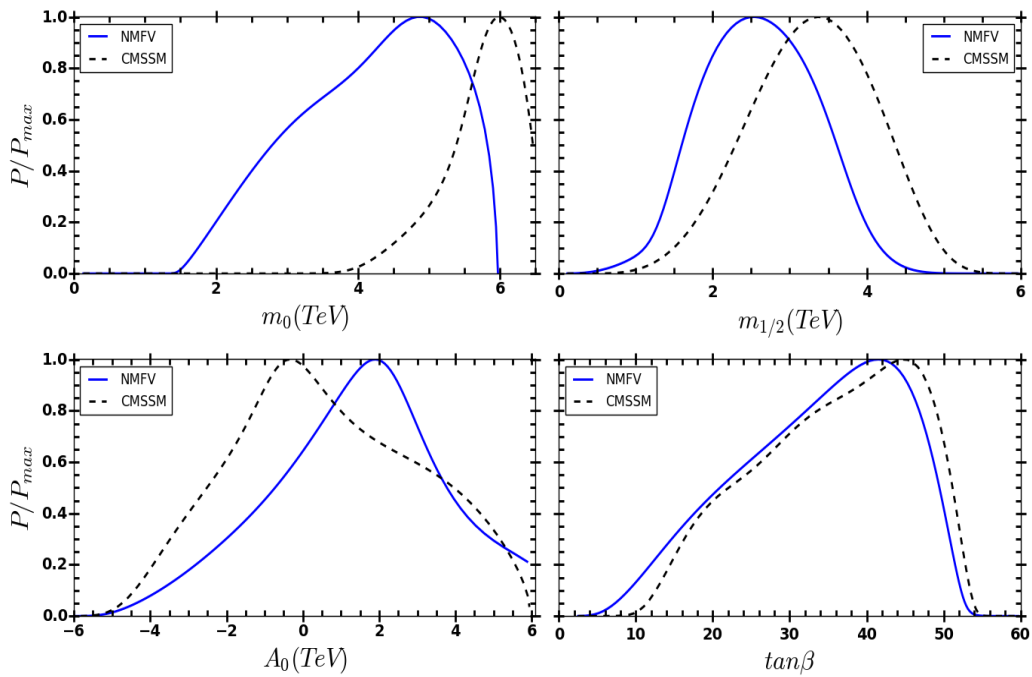


Figure 2: Posterior probability distributions of CMSSM parameters taking into account the constraints of LEP data, Higgs observables, precision observables, and the relic density of the dark matter using flat priors. The blue solid line illustrates the NMFV while the black dashed line depicts the CMSSM.

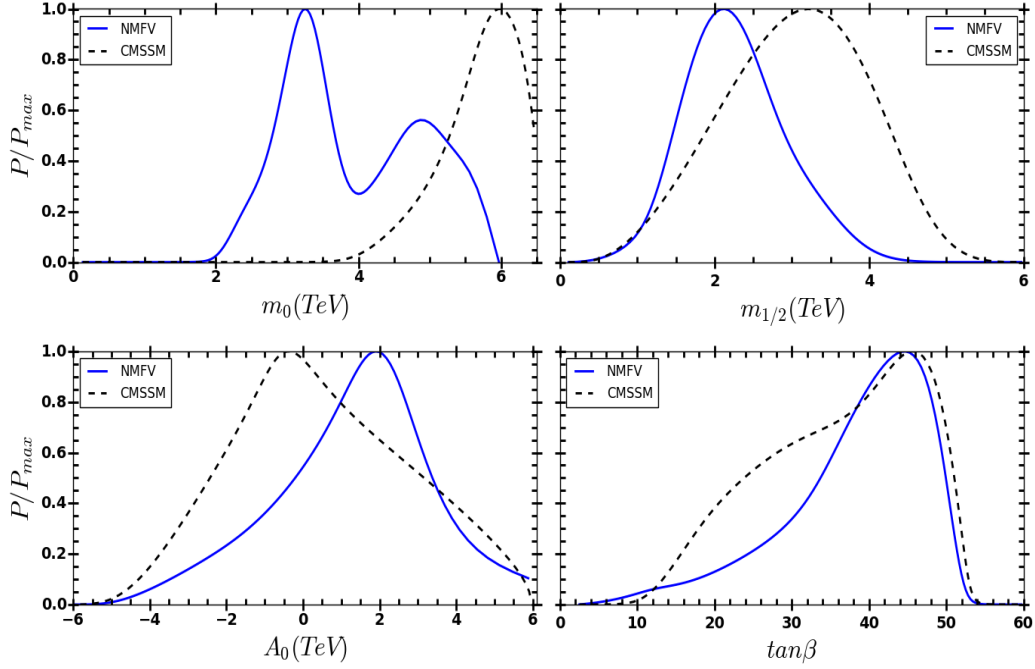


Figure 3: Posterior probability distributions of CMSSM parameters involving the constraints of LEP data, Higgs observables, precision observables, and the relic density of the dark matter utilising natural priors. The colour convention follows the same as in Figure 2.

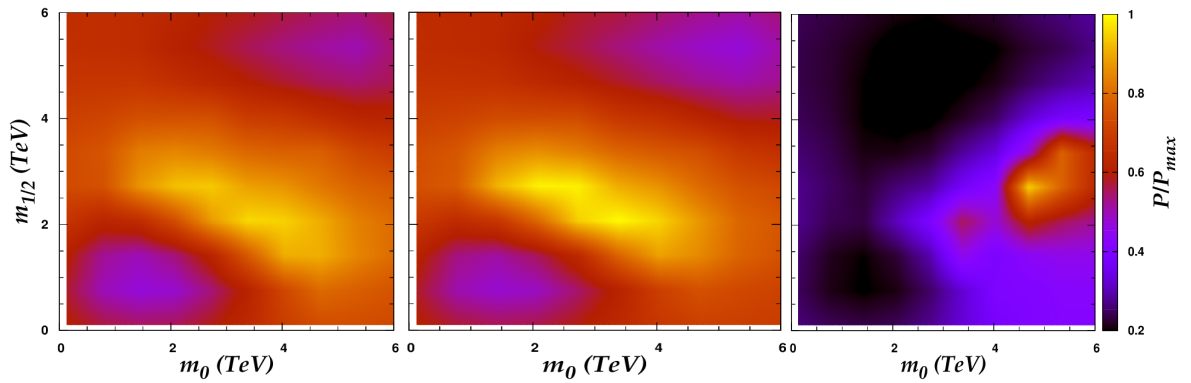


Figure 4: Heatmaps of m_0 , $m_{1/2}$ and posterior probability with flat priors for LEP+HO (left), LEP+HO+PO (middle), and LEP+HO+PO+DM (right) constraints in the LR sector of the scharm-stop flavour-violating interaction of the NMFV framework.

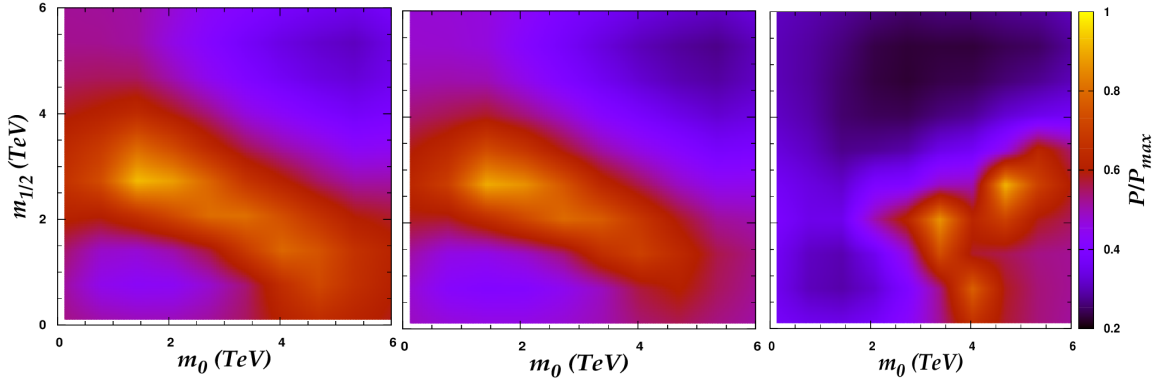


Figure 5: Heatmaps of $m_0, m_{1/2}$ and posterior probability with natural priors for LEP+HO (left), LEP+HO+PO (middle), and LEP+HO+PO+DM (right) constraints in the LR sector of the scharm-stop flavour-violating interaction of the NMFV framework.

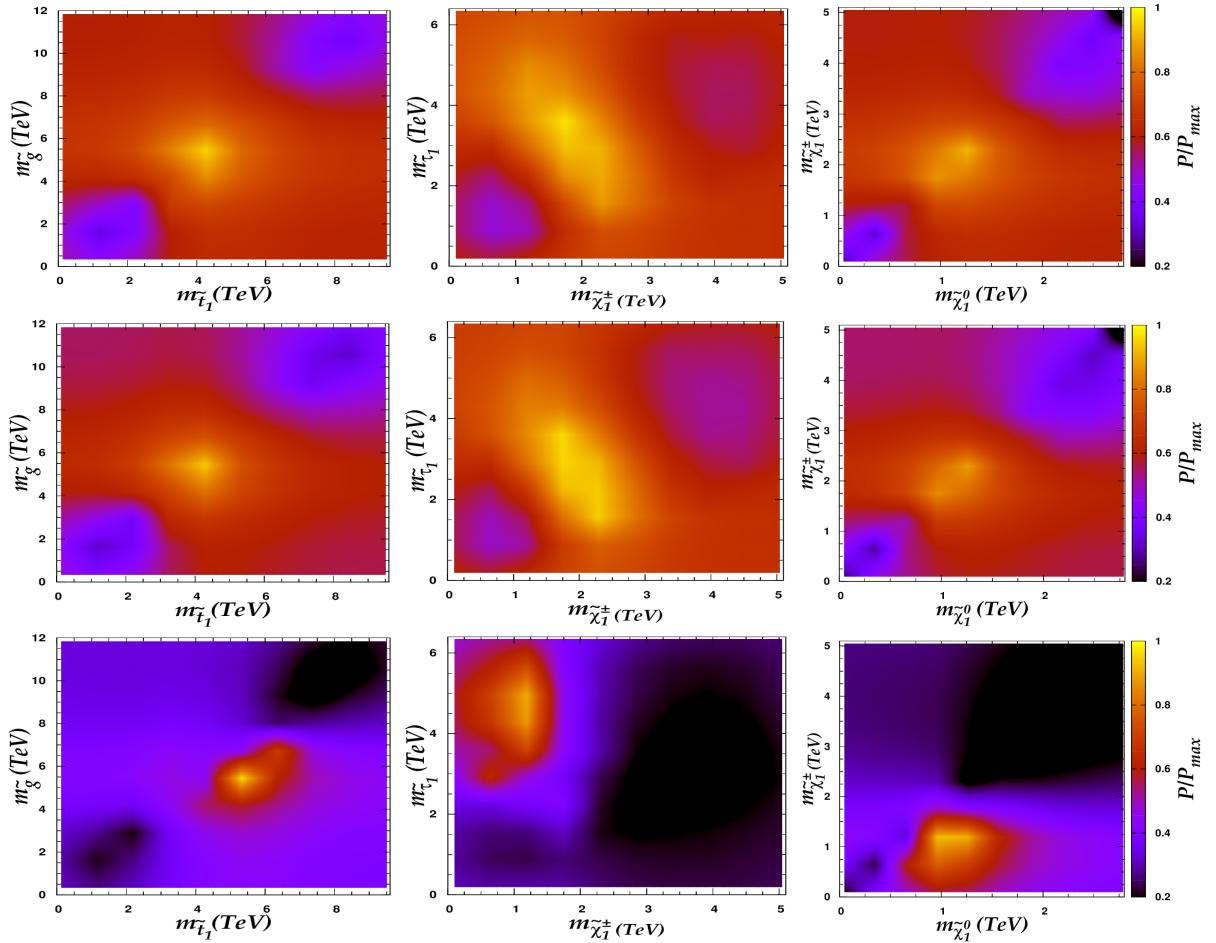


Figure 6: Heatmaps of particles masses with posterior probability for three different sets of constraints i.e. LEP+HO (first row), LEP+HO+PO (second row), and LEP+HO+PO+DM (third row) constraints in the NMFV framework using flat priors.

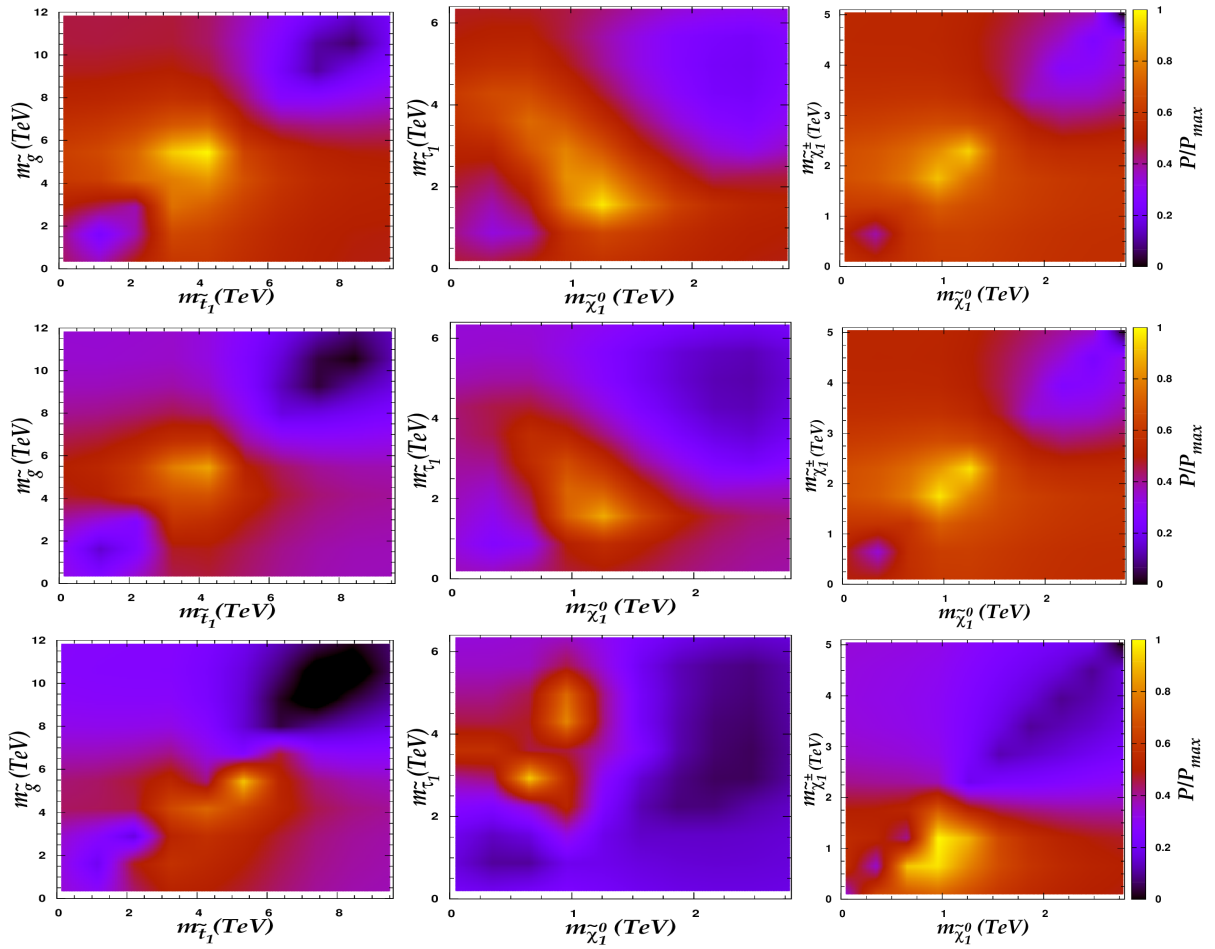


Figure 7: Heatmaps of sparticles masses with posterior probability for three different sets of constraints in the NMFV framework using natural priors. The convention follows the same as in Figure 6.

Parameter	Flat priors			Natural priors		
	LEP+HO	+PO	+DM	LEP+HO	+PO	+DM
m_0	4.06	3.63	4.83	1.48	1.59	3.25
$m_{1/2}$	2.42	2.36	2.54	2.39	2.34	2.13
A_0	-5.18	-4.68	1.90	-5.28	-5.00	1.90
$\tan\beta$	10.7	40.3	41.5	26.4	36.7	44.7
δ_{ct}^{LR}	4.4×10^{-2}	5×10^{-2}	6.1×10^{-2}	5.5×10^{-2}	5.5×10^{-2}	5.9×10^{-2}
m_H	3.33	3.33	2.05	3.33	3.14	2.06
m_{A^0}	3.52	3.33	2.04	3.33	3.23	2.04
m_{H^\pm}	3.54	3.24	2.06	3.24	3.24	2.06
$m_{\tilde{\chi}_1^0}$	1.02	1.05	1.04	1.09	1.05	0.95
$m_{\tilde{\chi}_2^0}$	1.96	1.96	1.09	1.96	1.96	1.09
$m_{\tilde{\chi}_3^0}$	2.60	2.60	1.69	2.60	2.60	1.46
$m_{\tilde{\chi}_4^0}$	2.51	2.51	1.93	2.51	2.51	1.93
$m_{\tilde{\chi}_1^\pm}$	1.96	1.96	1.07	2.00	2.00	1.04
$m_{\tilde{\chi}_2^\pm}$	2.62	2.52	1.93	2.52	2.52	1.93
$m_{\tilde{g}}$	4.94	4.94	5.57	4.94	4.94	4.54
$m_{\tilde{q}_L}$	5.06	4.95	7.13	4.84	4.84	4.63
$m_{\tilde{q}_R}$	4.85	4.85	7.00	4.75	4.75	4.59
$m_{\tilde{b}_1}$	4.34	4.34	5.95	4.34	4.34	3.98
$m_{\tilde{b}_2}$	4.46	4.46	6.66	4.46	4.46	4.08
$m_{\tilde{t}_1}$	3.88	3.88	5.14	3.74	3.79	3.55
$m_{\tilde{t}_2}$	4.36	4.36	5.95	4.36	4.36	3.89
$m_{\tilde{t}_L}$	3.34	3.07	5.71	2.63	2.63	3.46
$m_{\tilde{t}_R}$	3.92	2.85	5.64	1.92	1.92	3.32
$m_{\tilde{\tau}_1}$	3.79	1.95	4.62	1.49	1.49	2.47
$m_{\tilde{\tau}_2}$	3.01	2.68	4.76	2.44	2.44	2.91

Table 4: The sparticle mass spectrum at maximum posterior probability for NMFV framework in the LR sector of the scharm-stop flavour-violating interaction with flat and natural priors respectively. All mass parameters are in TeV except $\tan\beta$ and δ_{ct}^{LR} which are dimensionless.

particles, where the NMFV scenario favours lighter masses for SUSY particles than the base model CMSSM. The Bayes factors as presented in Table 3 for our model turn out to be about 5.73 with flat priors and 6.01 with natural priors on the logarithmic Jeffreys scale. While CMSSM has been taken to be the base model which obviously corresponds to “decisive” evidence on Jeffreys scale. Our work reveals that the most probable values of the neutralino LSP, corresponding to the flat and natural priors, are found to be around 1.04 TeV and 0.95 TeV, respectively. It would be preferable to consider this effect at the LHC to meet the signatures of SUSY in the future.

Acknowledgments

We thank Csaba Balazs for critical reading, discussions and valuable comments throughout the span of this work. This work was supported in part by University Grants Com-

mission (UGC) under a Start-Up Grant no. F30-377/2017 (BSR). We acknowledge the use of computing facility at the DST computational lab of the Physics Department, AMU, Aligarh during the early phase of the work.

References

- [1] A. Djouadi, Phys. Rept. **457**, 1-216 (2008), [arXiv:hep-ph/0503172 [hep-ph]].
- [2] G. Aad *et al.* [ATLAS and CMS], Phys. Rev. Lett. **114**, 191803 (2015), [arXiv:1503.07589 [hep-ex]].
- [3] G. L. Kane, C. F. Kolda, L. Roszkowski and J. D. Wells, Phys. Rev. D **49**, 6173-6210 (1994), [arXiv:hep-ph/9312272 [hep-ph]].
- [4] B. C. Allanach, K. Cranmer, C. G. Lester and A. M. Weber, JHEP **08**, 023 (2007), [arXiv:0705.0487 [hep-ph]].
- [5] C. Balazs, A. Buckley, D. Carter, B. Farmer and M. White, Eur. Phys. J. C **73**, 2563 (2013), [arXiv:1205.1568 [hep-ph]].
- [6] A. Fowlie, M. Kazana, K. Kowalska, S. Munir, L. Roszkowski, E. M. Sessolo, S. Trojanowski and Y. L. S. Tsai, Phys. Rev. D **86**, 075010 (2012), [arXiv:1206.0264 [hep-ph]].
- [7] P. Athron, C. Balazs, B. Farmer, A. Fowlie, D. Harries and D. Kim, JHEP **10**, 160 (2017), [arXiv:1709.07895 [hep-ph]].
- [8] P. Athron *et al.* [GAMBIT], Eur. Phys. J. C **77**, no.12, 824 (2017), [arXiv:1705.07935 [hep-ph]].
- [9] J. Ellis, J. L. Evans, F. Luo, K. A. Olive and J. Zheng, Eur. Phys. J. C **78**, no.5, 425 (2018), [arXiv:1801.09855 [hep-ph]].
- [10] M. Drees, [arXiv:hep-ph/9611409 [hep-ph]].
- [11] S. P. Martin, Adv. Ser. Direct. High Energy Phys. **21**, 1-153 (2010), [arXiv:hep-ph/9709356 [hep-ph]].
- [12] X. Tata, [arXiv:hep-ph/9706307 [hep-ph]].
- [13] D. J. H. Chung, L. L. Everett, G. L. Kane, S. F. King, J. D. Lykken and L. T. Wang, Phys. Rept. **407**, 1-203 (2005), [arXiv:hep-ph/0312378 [hep-ph]].
- [14] I. J. R. Aitchison, [arXiv:hep-ph/0505105 [hep-ph]].
- [15] A. Djouadi, Phys. Rept. **459**, 1-241 (2008), [arXiv:hep-ph/0503173 [hep-ph]].
- [16] P. Fayet, Adv. Ser. Direct. High Energy Phys. **26**, 397-454 (2016), [arXiv:1506.08277 [hep-ph]].
- [17] B. C. Allanchach, CERN Yellow Rep. School Proc. **6**, 113-144 (2019).

- [18] A. Canepa, *Rev. Phys.* **4**, 100033 (2019).
- [19] C. Balázs and S. K. Gupta, *Phys. Rev. D* **87**, no.3, 035023 (2013), [arXiv:1212.1708 [hep-ph]].
- [20] S. Heinemeyer, W. Hollik, F. Merz and S. Penaranda, *Eur. Phys. J. C* **37**, 481-493 (2004), [arXiv:hep-ph/0403228 [hep-ph]].
- [21] G. Bozzi, B. Fuks, B. Herrmann and M. Klasen, *Nucl. Phys. B* **787**, 1-54 (2007), [arXiv:0704.1826 [hep-ph]].
- [22] M. Arana-Catania, S. Heinemeyer, M. J. Herrero and S. Penaranda, *JHEP* **05**, 015 (2012), [arXiv:1109.6232 [hep-ph]].
- [23] M. Arana-Catania, S. Heinemeyer, M. J. Herrero and S. Penaranda, [arXiv:1201.6345 [hep-ph]].
- [24] M. Arana-Catania, S. Heinemeyer and M. J. Herrero, *Phys. Rev. D* **90**, no.7, 075003 (2014), [arXiv:1405.6960 [hep-ph]].
- [25] J. Bernigaud, B. Herrmann, S. F. King and S. J. Rowley, *JHEP* **03**, 067 (2019), [arXiv:1812.07463 [hep-ph]].
- [26] K. Kowalska, *JHEP* **09**, 139 (2014), [arXiv:1406.0710 [hep-ph]].
- [27] J. Bernigaud and B. Herrmann, *SciPost Phys.* **6**, no.6, 066 (2019), [arXiv:1809.04370 [hep-ph]].
- [28] K. De Causmaecker, B. Fuks, B. Herrmann, F. Mahmoudi, B. O’Leary, W. Porod, S. Sekmen and N. Strobbe, *JHEP* **11**, 125 (2015), [arXiv:1509.05414 [hep-ph]].
- [29] M. Carena, A. Menon, R. Noriega-Papaqui, A. Szykman and C. E. M. Wagner, *Phys. Rev. D* **74**, 015009 (2006), [arXiv:hep-ph/0603106 [hep-ph]].
- [30] F. del Aguila, J. A. Aguilar-Saavedra, B. C. Allanach, J. Alwall, Y. Andreev, D. Ariztizabal Sierra, A. Bartl, M. Beccaria, S. Bejar and L. Benucci, *et al.*, *Eur. Phys. J. C* **57**, 183-308 (2008). [arXiv:0801.1800 [hep-ph]].
- [31] M. Bruhnke, B. Herrmann and W. Porod, *JHEP* **09**, 006 (2010), [arXiv:1007.2100 [hep-ph]].
- [32] B. Herrmann, M. Klasen and Q. Le Boulc’h, *Phys. Rev. D* **84**, 095007 (2011), [arXiv:1106.6229 [hep-ph]].
- [33] T. Hahn, W. Hollik, J. I. Illana and S. Penaranda, [arXiv:hep-ph/0512315 [hep-ph]].
- [34] B. Fuks, B. Herrmann and M. Klasen, *Nucl. Phys. B* **810**, 266-299 (2009), [arXiv:0808.1104 [hep-ph]].
- [35] B. Fuks, B. Herrmann and M. Klasen, *Phys. Rev. D* **86**, 015002 (2012), [arXiv:1112.4838 [hep-ph]].

- [36] Q. Y. Hu, X. Q. Li, Y. D. Yang and M. D. Zheng, JHEP **06**, 133 (2019), [arXiv:1903.06927 [hep-ph]].
- [37] S. Gupta and S. K. Gupta, Nucl. Phys. B **984**, 115942 (2022), [arXiv:2205.00173 [hep-ph]].
- [38] G. Hiller, Y. Hochberg and Y. Nir, JHEP **03**, 115 (2009), [arXiv:0812.0511 [hep-ph]].
- [39] J. Guasch and J. Sola, Nucl. Phys. B **562**, 3-28 (1999), [arXiv:hep-ph/9906268 [hep-ph]].
- [40] J. Cao, G. Eilam, K. i. Hikasa and J. M. Yang, Phys. Rev. D **74**, 031701 (2006), [arXiv:hep-ph/0604163 [hep-ph]].
- [41] J. J. Cao, G. Eilam, M. Frank, K. Hikasa, G. L. Liu, I. Turan and J. M. Yang, Phys. Rev. D **75**, 075021 (2007), [arXiv:hep-ph/0702264 [hep-ph]].
- [42] A. M. Curiel, M. J. Herrero and D. Temes, Phys. Rev. D **67**, 075008 (2003), [arXiv:hep-ph/0210335 [hep-ph]].
- [43] A. M. Curiel, M. J. Herrero, W. Hollik, F. Merz and S. Penaranda, Phys. Rev. D **69**, 075009 (2004), [arXiv:hep-ph/0312135 [hep-ph]].
- [44] S. Bejar, F. Dilme, J. Guasch and J. Sola, JHEP **08**, 018 (2004), [arXiv:hep-ph/0402188 [hep-ph]].
- [45] D. Atwood, S. K. Gupta and A. Soni, JHEP **10**, 057 (2014), [arXiv:1305.2427 [hep-ph]].
- [46] P. A. Zyla *et al.* [Particle Data Group], Prog. Theor. Exp. Phys. **2020**, no.8, 083C01 (2020).
- [47] B. C. Allanach, Comput. Phys. Commun. **143**, 305-331 (2002), [arXiv:hep-ph/0104145 [hep-ph]].
- [48] S. Heinemeyer, W. Hollik and G. Weiglein, Eur. Phys. J. C **9**, 343-366 (1999), [arXiv:hep-ph/9812472 [hep-ph]].
- [49] S. Heinemeyer, W. Hollik and G. Weiglein, Comput. Phys. Commun. **124**, 76-89 (2000), [arXiv:hep-ph/9812320 [hep-ph]].
- [50] G. Degrossi, S. Heinemeyer, W. Hollik, P. Slavich and G. Weiglein, Eur. Phys. J. C **28**, 133-143 (2003), [arXiv:hep-ph/0212020 [hep-ph]].
- [51] M. Frank, T. Hahn, S. Heinemeyer, W. Hollik, H. Rzehak and G. Weiglein, JHEP **02**, 047 (2007), [arXiv:hep-ph/0611326 [hep-ph]].
- [52] T. Hahn, S. Heinemeyer, W. Hollik, H. Rzehak and G. Weiglein, Phys. Rev. Lett. **112**, no.14, 141801 (2014), [arXiv:1312.4937 [hep-ph]].
- [53] H. Bahl and W. Hollik, Eur. Phys. J. C **76**, no.9, 499 (2016), [arXiv:1608.01880 [hep-ph]].

- [54] H. Bahl, S. Heinemeyer, W. Hollik and G. Weiglein, *Eur. Phys. J. C* **78**, no.1, 57 (2018), [arXiv:1706.00346 [hep-ph]].
- [55] H. Bahl, T. Hahn, S. Heinemeyer, W. Hollik, S. Paßehr, H. Rzehak and G. Weiglein, *Comput. Phys. Commun.* **249**, 107099 (2020), [arXiv:1811.09073 [hep-ph]].
- [56] A. Arbey, F. Mahmoudi and G. Robbins, *Comput. Phys. Commun.* **239**, 238-264 (2019), [arXiv:1806.11489 [hep-ph]].
- [57] G. Belanger, F. Boudjema, A. Pukhov and A. Semenov, *Comput. Phys. Commun.* **174**, 577-604 (2006), [arXiv:hep-ph/0405253 [hep-ph]].
- [58] G. Belanger, F. Boudjema, A. Pukhov and A. Semenov, *Comput. Phys. Commun.* **149**, 103-120 (2002), [arXiv:hep-ph/0112278 [hep-ph]].
- [59] S. Schael *et al.* [ALEPH, DELPHI, L3, OPAL and LEP Working Group for Higgs Boson Searches], *Eur. Phys. J. C* **47**, 547-587 (2006), [arXiv:hep-ex/0602042 [hep-ex]].
- [60] B. Abi *et al.* [Muon g-2], *Phys. Rev. Lett.* **126**, no.14, 141801 (2021), [arXiv:2104.03281 [hep-ex]].
- [61] Y. S. Amhis *et al.* [HFLAV], *Eur. Phys. J. C* **81**, no.3, 226 (2021), [arXiv:1909.12524 [hep-ex]].
- [62] P. A. R. Ade *et al.* [Planck], *Astron. Astrophys.* **594**, A13 (2016), [arXiv:1502.01589 [astro-ph.CO]].